

Controlling 3D spin textures by manipulating sign and amplitude of interlayer DMI with electrical current

Fabian Kammerbauer¹, Won-Young Choi^{1,2}, Frank Freimuth^{1,3}, Kyujoon Lee⁴,
Robert Frömter¹, Dong-Soo Han², Henk J. M. Swagten⁵, Yuriy Mokrousov^{1,3}
and Mathias Kläui¹

1 Institute of Physics, Johannes Gutenberg-Universität Mainz, Mainz, Germany

2 Center for Spintronics, Korea Institute of Science and Technology, Seoul,
Republic of Korea

3 Peter Grünberg Institut and Institute for Advanced Simulation,
Forschungszentrum Jülich and JARA, Jülich, Germany

4 Division of display and semiconductor physics, Korea University, Sejong,
Republic of Korea

5 Department of Applied Physics, Institute for Photonic Integration, Eindhoven
University of Technology, Eindhoven, The Netherlands

Abstract

The recently discovered interlayer Dzyaloshinskii-Moriya interaction (IL-DMI) in multilayers with perpendicular magnetic anisotropy favors the canting of spins in the in-plane direction and could thus enable new exciting spin textures such as Hopfions in continuous multilayer films. A key requirement is to control the IL-DMI and so in this study, the influence of an electric current on the IL-DMI is investigated by out-of-plane hysteresis loops of the anomalous Hall effect under applied in-plane magnetic fields. The direction of the in-plane field is varied to obtain a full azimuthal dependence, which allows us to quantify the effect on the IL-DMI. We observe a shift in the azimuthal dependence of the IL-DMI with increasing current, which can be understood from the additional in-plane symmetry breaking introduced by the current flow. Using an empirical model of two superimposed cosine functions we demonstrate the presence of a current-induced term that linearly increases the IL-DMI in the direction of current flow. With this, a new easily accessible possibility to manipulate 3D spin textures by current is realized. As most spintronic devices employ spin-transfer or spin-orbit torques to manipulate spin textures, the foundation to implement current-induced IL-DMI into thin-film devices is broadly available.

1 Introduction

The burgeoning field of 3D magnetism has introduced ways of bending and forming magnetic structures to ones will and produced magnetic nanoparticles [1], magnetic tubes [2] and more [3, 4]. Each with the distinct feature of manipulating the material itself towards its use in the third dimension. Another approach towards 3D magnetism are 3D topological textures within the magnetic system itself [3]. These new 3D spin structures, such as hopfions [5], offer advanced options for future spintronic applications [3, 4]. Compared to 2D spin structures, e.g. skyrmions stabilized by the Dzyaloshinskii-Moriya interaction (DMI) [6], it is more challenging to stabilize twisted spin configurations in the third dimension. The recently experimentally observed magnetic Hopfion uses a combination of strong DMI and the confinement in a nanodisk [5].

Another route towards Hopfions is offered by the antisymmetric interlayer exchange interaction, which has been termed as interlayer DMI (IL-DMI) [7–10]. It favors spin canting between layers in the lateral direction and originates from an in-plane symmetry breaking. This allows for a highly sought-after tuning mechanism for 3D magnetic textures, which could stabilize such structures in magnetic multilayers without confinement. The absence of confinement opens the possibility to move or aggregate these structures. While it is interesting to study the internal dynamics under the application of fields or currents [11] a possibility to directly control the IL-DMI strength can additionally provide direct access to internal transformations between different 3D magnetic textures. This would allow for writing and deleting operations, which are necessary when employing the different magnetic textures as bits. Conventionally, the strength of both the DMI and the IL-DMI is set during sample growth. For DMI post-growth changes to its magnitude have been shown, while for the IL-DMI these are elusive so far. One possible option to influence the DMI is strain. It has been shown that strain

can enhance the DMI [12, 13] and be used to tune the diameter of skyrmions [14]. A technologically more easily accessible option is applying an electrical field, which is typically used to introduce spin-transfer torques and spin-orbit torques in many systems [15–18] and has been recently shown to directly influence the strength of the conventional DMI [19–21]. The benefit of this approach is the direct tuning parameter allowing one to locally change the DMI and therefore the spin structures can be dynamically controlled.

So far, no tuning of the IL-DMI after growth has been reported but it is a key step towards using this effect. The goal of this study is to investigate possible effects on the IL-DMI induced by electrical currents. This will be a more direct and locally accessible tuning parameter for the IL-DMI rather than the global in-plane symmetry breaking or varying the spin-orbit-coupling by a different material choice, which cannot be changed after growth. Following this thought, this study investigates the influence of an electrical current on the IL-DMI by employing asymmetric hysteresis loop measurements, a technique we introduced earlier to demonstrate the presence of the IL-DMI [7]. We use symmetry arguments to explain that a chiral Néel-type state requires a gradient along the direction $(\mathbf{M}_1 \times \mathbf{M}_2) \times \mathbf{R}$, where \mathbf{R} is the distance vector between the magnetizations \mathbf{M}_1 and \mathbf{M}_2 of the two layers. When this gradient is provided by an applied electric field, several mechanisms for IL-DMI become possible. One mechanism is the spin Hall effect, which extends the spin-current picture of equilibrium DMI [22, 23] into the nonequilibrium regime.

2 Sample preparation

The investigated sample is a synthetic antiferromagnet (SAF) of Ta(4)/Pt(4)/Co(0.6)/Pt(0.7)/Ru(0.8)/Pt(0.5)/Co(1)/Pt(4) structure on Si/SiO₂ (layer thicknesses in nanometers). The two ferromagnetic (FM) layers, FM1 at the bottom

and FM2 at the top, are antiferromagnetically coupled across the Ru layer via the Ruderman-Kittel-Kasuya-Yosida (RKKY) interaction. The in-plane symmetry breaking necessary to give rise to the IL-DMI [7, 8], is introduced randomly during the sputtering process for this sample. The film was patterned into Hall bars by electron-beam lithography to allow for higher current densities compared to a continuous-film measurement.

3 Method

To investigate the IL-DMI, the method devised by Han et al. [7] was employed. For the case of a sample with IL-DMI and perpendicular magnetic anisotropy (PMA) the magnetization switching by an out-of-plane (OOP) field sweep will be supported or hindered in the presence of an in-plane bias field depending on its direction and the chirality of the DMI [24]. Similarly, in SAFs with PMA and IL-DMI, the magnetization switching is supported or hindered under application of an in-plane field depending on its azimuthal direction with respect to the in-plane symmetry breaking axis and the chirality introduced by the IL-DMI. Hysteresis loops obtained by sweeping the OOP field were measured by the anomalous Hall effect (AHE) in the patterned Hall bars while applying an in-plane field of 100 mT along a varied direction ϕ . The structure of the connections for the AHE setup are shown in fig. 1a). Two resulting hysteresis loops are presented in fig. 1b). The switching fields are derived from the hysteresis curve by fitting error functions to the data. The experimental uncertainty for all obtained switching-field values is primarily given by the step size of 0.5 mT for the hysteresis loops. The obtained switching fields can be determined separately for the two magnetic layers as the different thicknesses yield different signal height. In addition the two distinct sweep directions up-to-down (U-D) and down-to-up (D-U), with up and down positive and negative field in z-direction, are considered separately. By varying

ϕ in steps of 30° a full azimuthal dependence is obtained. This allows us to find the direction of the axis of the antisymmetric behaviour, which is the direction where the asymmetry between U-D and D-U switching fields is the largest, as shown in fig. 1c) and d). There the antisymmetric axis points approximately along 240° . The presence of an antisymmetric axis indicates the presence of IL-DMI in this sample.

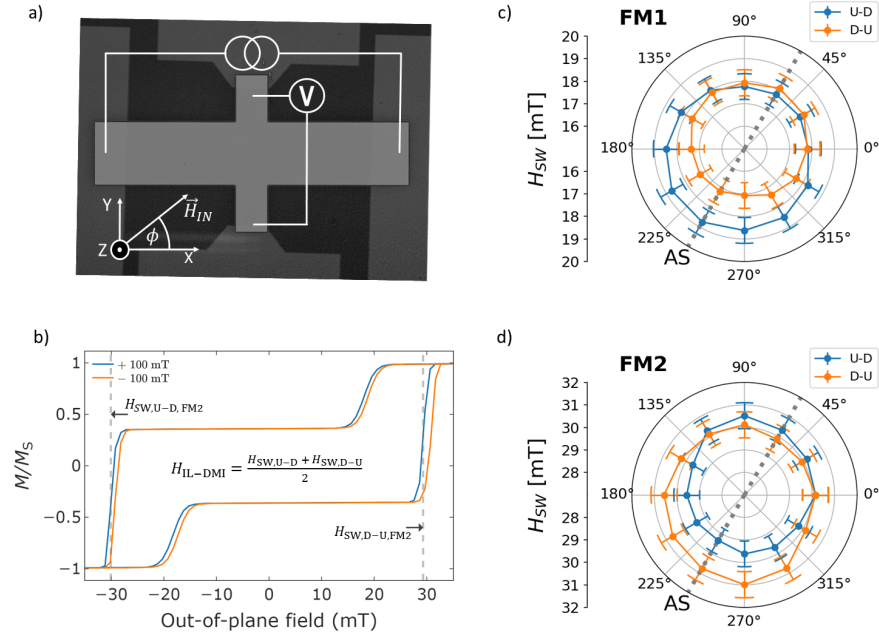


Figure 1: a) Hall-bar structure with indicated connections. For the anomalous Hall effect measurements a dc current along $+x$ direction is applied while sweeping the out-of-plane field in z -direction. Additionally, an in-plane field \vec{H}_{IN} of 100 mT is applied along an angle ϕ , with ϕ varying from 0° to 330° in 30° steps. b) Magnetic hysteresis loops measured by anomalous Hall effect. Blue and orange curves display the hysteresis under the influence of positive and negative in-plane field of 100 mT, respectively, which was aligned along the antisymmetric axis. The difference between the two switching fields can be defined as a bias field H_{IL-DMI} originating from the IL-DMI. c) and d) display the dependence of the switching fields on the in-plane field angle ϕ for FM1 and FM2 respectively measured at the lowest current density of $0.6 \times 10^9 \text{ A/m}^2$. The antisymmetric axis (AS) is indicated by a grey dotted line.

4 Results

To quantify and compare the IL-DMI for several current densities we assume the IL-DMI to act as a bias field that shifts the hysteresis loop, as we have seen in fig. 1b). This effect can be quantified by an IL-DMI field, which we name $H_{\text{IL-DMI}}$. We define $H_{\text{IL-DMI}}$ as the difference between the U-D and D-U switching fields divided by two, similar to [10].

$$H_{\text{IL-DMI}} = \frac{H_{\text{SW,U-D}} + H_{\text{SW,D-U}}}{2} \quad (1)$$

with $H_{\text{SW,U-D}}$ and $H_{\text{SW,D-U}}$ the switching fields for U-D and D-U switching, respectively, as illustrated in fig. 1b). This description assumes that there are no other bias effects leading to asymmetric hysteresis loops, such as exchange bias [25, 26] or biquadratic interlayer exchange interaction effects [27]. Figure 2 presents the values of the $H_{\text{IL-DMI}}$ field as function of ϕ for the two different ferromagnetic layers for the lowest and highest current densities. The sinusoidal dependence on the angle is the fingerprint for the presence of an IL-DMI, as the latter is directly dependent on the angle between the applied field and the in-plane inversion symmetry breaking, i.e., the antisymmetric axis. We can exclude any effect from biquadratic interlayer exchange, which would be isotropic in nature [28], same with the DMI, which is symmetric in the field direction, i.e., $H_{\text{SW}}(-\phi) = H_{\text{SW}}(\phi)$ [24]. Therefore, we can conclude that the IL-DMI is the origin of the shift of the hysteresis curves at low and high current densities.

Next, we study the current-dependence of the $H_{\text{IL-DMI}}$ for FM1 and FM2 as shown in fig. 2. There is a slight increase in the amplitude of $H_{\text{IL-DMI}}$, as well as a shift in the maximum position of the fitted sine function. The shift in the asymmetric axis indicates a change in the in-plane inversion symmetry breaking. The latter is usually related to an asymmetric growth or thickness

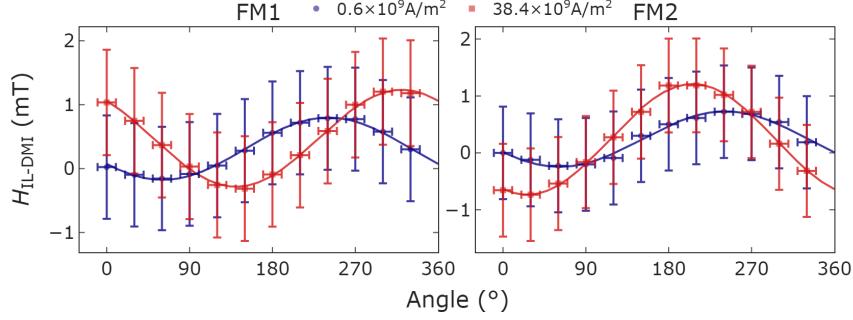


Figure 2: Azimuthal dependence of IL-DMI for the lowest current density at $0.6 \times 10^9 \text{ A/m}^2$ and the highest current density at $38.4 \times 10^9 \text{ A/m}^2$, for FM1 on the left and FM2 on the right. The lines are sine fits to the data.

gradient [7]. The application of a current should intrinsically break the in-plane inversion symmetry as the electrons move in a defined direction within the Hall-bar. Meaning when the current effect is significantly large it could change the direction of the in-plane symmetry breaking. Therefore, we can assume that any applied electrical current yields an additional term to the IL-DMI that is oriented along the direction of electrical current and can be described by a cosine function. To investigate this statement we devised a simple model of two superimposed cosine functions, one static, governed by the geometry of the sample and its intrinsic inversion-symmetry breaking, and a second one for the current-induced effect. We thus use the following model for a shared-parameter fit.

$$H_{\text{IL-DMI}} = a_0 \cos(\phi - \phi_0) + a_j \cos(\phi - \phi_j) + b, \quad (2)$$

with ϕ the angle of the applied field, ϕ_0 the angular direction of symmetry breaking defined by the sample growth, i.e., the maximum position of $H_{\text{IL-DMI}}$ at zero applied current, ϕ_j the azimuthal direction of the current-induced IL-DMI, a_0 and a_j are the amplitudes and b is an offset. Note that the positive current

direction is along 0° (see fig. 1). We assume the first term to be independent of current, thereby, ϕ_0 is fixed along the direction of the antisymmetric axis and is determined by extrapolating sine fits of the data to the zero current limit which yields $241 \pm 3^\circ$ for the case of FM1 and $243 \pm 4^\circ$ for FM2. Furthermore, we assume ϕ_j to align with the current direction, i.e., towards 0° for positive current. Using eq. (2) the data of $H_{\text{IL-DMI}}$ for all available current densities is fitted. We expect the parameters a_0 and ϕ_j to be constant for all current densities, as long as the direction of the current does not change. Therefore, we employ a shared-parameter fit, where ϕ_j & a_0 are shared parameters. We fix the value of ϕ_0 to obtain a_j , which is not a shared parameter as we expect it to increase with current density. The resulting values of ϕ_j & a_0 are shown in table 1 and show ϕ_j to point approximately along 0° , i.e., the current direction. The trend of a_j with current density shows a linear increase, see fig. 3a), however, the slope is positive for FM1 and negative for FM2, see slope in table 1. A slight increase for the slope at higher current densities might be related to an increase in temperature due to Joule heating.

current	layer	ϕ_j ($^\circ$)	a_0 (mT)	slope ($\mu\text{T}/10^9\text{Am}^{-2}$)
+	FM1	-4.9 ± 0.8	0.48 ± 0.01	18.1 ± 0.3
+	FM2	2.9 ± 2.3	0.48 ± 0.01	-8.6 ± 0.3

Table 1: Shared parameters across all positive current densities obtained from fitting the IL-DMI field to current densities. And slope of the linear fits shown in fig. 3a). The initial value for ϕ_j is 0° .

For better understanding of any possibly underlying asymmetry for FM1 and FM2, the measurement was repeated using positive and negative current polarities. If the proposed model is correct, then, due to reversal of the current direction, ϕ_j should align towards 180° while a_j stays of similar magnitude. And indeed, the shared parameter ϕ_j follows an alignment towards 180° for negative current polarity, compare with table 2. And a_j displays similar size

for positive and negative fields within the investigated current density range, as shown in fig. 3b). The slopes of the linear fits displayed in fig. 3b) are presented in table 2. The nature of this observation can be better understood when employing symmetry arguments. We may write the IL-DMI energy associated with the chiral state as $F = (\mathbf{T}_2 - \mathbf{T}_1) \cdot (\mathbf{M}_1 \times \mathbf{M}_2)$, where \mathbf{M}_1 and \mathbf{M}_2 are the magnetizations in FM1 and FM2, respectively, and \mathbf{T}_i is the contribution to the torque on M_i that stems from the IL-DMI (the total torque is zero in the stationary state). These torques \mathbf{T}_i need to point into the direction of $\mathbf{M}_1 \times \mathbf{M}_2$ in order to produce a contribution to F (with $\mathbf{T}_1 \neq \mathbf{T}_2$). If the system contains a mirror plane that flips the sign of $\mathbf{M}_1 \times \mathbf{M}_2$, it therefore also flips the relevant component of $(\mathbf{T}_2 - \mathbf{T}_1)$ without changing the energy F , which is inconsistent with the DMI interaction that changes sign, when $\mathbf{M}_1 \times \mathbf{M}_2$ changes sign. This mirror plane may be eliminated by a material gradient or an applied electric current in the direction $(\mathbf{M}_1 \times \mathbf{M}_2) \times \mathbf{R}$, where \mathbf{R} is the distance vector between the two ferromagnetic vectors. The injection of spin current from the SHE into the ferromagnetic layers may generate these torques \mathbf{T}_2 and \mathbf{T}_1 . In this case one may understand the IL-DMI also from the balance equation of the torques and it is not necessary to consider the energy F : The torque balance equations on FM1 and FM2 may be written as $-J(\mathbf{M}_1 \times \mathbf{M}_2) + \mathbf{T}_1 = 0$ and $-J(\mathbf{M}_2 \times \mathbf{M}_1) + \mathbf{T}_2 = 0$, where J is the exchange coupling. By summing these two equations one obtains a single one: $2J(\mathbf{M}_1 \times \mathbf{M}_2) = \mathbf{T}_1 - \mathbf{T}_2$. Consequently, a chiral magnetic state characterized by the chirality $(\mathbf{M}_1 \times \mathbf{M}_2) \neq 0$ will occur when $\mathbf{T}_2 \neq \mathbf{T}_1$. In the samples considered it is likely that injection of spin current into the FM layers yields even different signs of \mathbf{T}_2 and \mathbf{T}_1 .

The change of the effect due to the current poality shows that the effect does not arise due to heating effects. To understand any effect heating may have on the sample, a continuous film of a similar sample system

current	layer	ϕ_j ($^\circ$)	a_0 (mT)	slope ($\mu\text{T}/10^9\text{A m}^{-2}$)
+	FM1	1.7 ± 0.4	0.43 ± 0.02	18.6 ± 0.9
+	FM2	171.7 ± 2.8	0.44 ± 0.04	-8.7 ± 2.9
-	FM1	-5 ± 20	0.40 ± 0.09	-20.2 ± 0.6
-	FM2	222 ± 13	0.62 ± 0.08	12.0 ± 2.8

Table 2: Shared parameters across all current densities obtained from fitting the IL-DMI field to positive and negative current densities from the additional measurement. The initial values for ϕ_j are -10° and 170° , for positive and negative currents respectively.

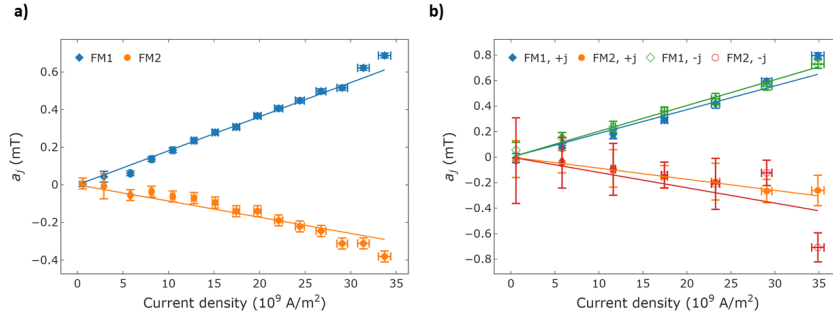


Figure 3: The current-induced contribution of the interlayer DMI a_j as function of current density. a), b) display data from two different measurement sets. The first set in a) displays the strict current dependence for both ferromagnetic layers. In the second set the current polarity dependence was investigated. The displayed data a_j is the amplitude of the current-induced part in the superimposed cosine fit as by eq. (2). The lines represent linear fits to data up to $30 \times 10^9 \text{ A/m}^2$.

Ta(4)/Pt(4)/Co(0.6)/Pt(0.5)/Ru(0.8)/Pt(0.5)/Co(1)/Pt(4), was investigated in a cryostat as function of temperature. The effect on the IL-DMI field for temperatures varying between 200 K and 300 K is present but small, see fig. 4. Additionally, the Joule heating in the Hall bar was simulated using COMSOL multiphysics, similar to an approach to estimate the heating in NiO/Pt systems [29]. The simulation yields a Joule heating of about 18 K for a current density of $38.4 \times 10^9 \text{ A/m}^2$. Considering the small dependence of IL-DMI on temperature, as seen in fig. 4, and the little effect of Joule heating, we can deduce Joule heating to play a negligible effect on the magnitude of the IL-DMI in our

sample.

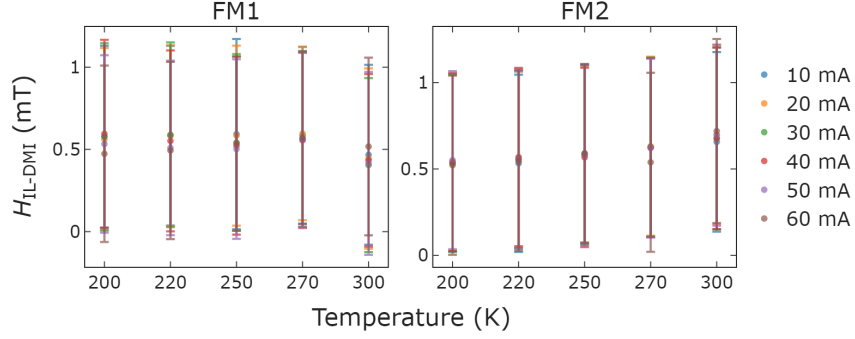


Figure 4: The IL-DMI field as function of temperature for a continuous film of Ta(4)/Pt(4)/Co(0.6)/Pt(0.5)/Ru(0.8)/Pt(0.5)/Co(1)/Pt(4) measured at various total currents.

5 Summary

In conclusion, the current dependence of the IL-DMI in SAFs has been found by studying the switching fields obtained from AHE measurements and quantified by means of the resulting IL-DMI field $H_{\text{IL-DMI}}$, which displays a significant shift in the azimuthal dependence for increasing current density. By employing a simple model of two superimposed cosine functions with a static and current-induced contribution, the observed behavior was reliably modeled. The fit yields a current-induced contribution for the IL-DMI, scaling linearly with current. The opposite current polarity reveals a consistent trend, with the opposite azimuthal dependence and similar amplitudes. From the symmetry point of view, an applied electric current along the direction $(\mathbf{M}_1 \times \mathbf{M}_2) \times \mathbf{R}$ – where \mathbf{R} is the distance vector between the magnetizations \mathbf{M}_1 and \mathbf{M}_2 of the two layers – allows for a chiral Néel-type state. One possible mechanism for the IL-DMI is the spin

Hall effect, which provides torques of opposite sign on the two magnetizations FM1 and FM2. The observed effect is conforming with the performed symmetry analysis, calling for future studies to also develop a quantitative theoretical model. The effect has the appearance of a purely current-induced effect, as growth dependent IL-DMI and current-induced IL-DMI superimpose. Therefore, we assume this effect to be present in systems without IL-DMI. Such a current-induced contribution to the IL-DMI allows for the highly desirable control of this chiral interaction and enables a direct, post-growth tuning mechanism for 3D topological spin structures in future spintronic devices.

6 Acknowledgements

F.K. acknowledges funding by the Deutsche Forschungsgemeinschaft (DFG, German Research Foundation) - TRR 173/2 - 268565370 Spin+X (Projects A01+B02). This project has received funding from the European Research Council (ERC) under the European Union's Horizon 2020 research and innovation programme (Grant No. 856538, project "3D MAGiC").

References

1. López-Ortega, A., Estrader, M., Salazar-Alvarez, G., Roca, A. G. & Nogués, J. Applications of exchange coupled bi-magnetic hard/soft and soft/hard magnetic core/shell nanoparticles. *Phys. Rep.* **553**, 1–32 (2015).
2. Streubel, R. *et al.* Retrieving spin textures on curved magnetic thin films with full-field soft X-ray microscopies. *Nat. Commun.* **6**, 7612 (2015).
3. Fischer, P., Sanz-Hernández, D., Streubel, R. & Fernández-Pacheco, A. Launching a new dimension with 3D magnetic nanostructures. *APL Mater.* **8**, 010701 (2020).

4. Fernández-Pacheco, A. *et al.* Three-dimensional nanomagnetism. *Nat. Commun.* **8**, 15756 (2017).
5. Kent, N. *et al.* Creation and observation of Hopfions in magnetic multilayer systems. *Nat. Commun.* **12**, 1562 (2021).
6. Fert, A., Cros, V. & Sampaio, J. Skyrmions on the track. *Nature Nanotechnol.* **8**, 152–156 (2013).
7. Han, D.-S. *et al.* Long-range chiral exchange interaction in synthetic antiferromagnets. *Nat. Mater.* **18**, 703–708 (2019).
8. Fernández-Pacheco, A. *et al.* Symmetry-breaking interlayer Dzyaloshinskii–Moriya interactions in synthetic antiferromagnets. *Nat. Mater.* **18**, 679–684 (2019).
9. Vedmedenko, E. Y., Riego, P., Arregi, J. A. & Berger, A. Interlayer Dzyaloshinskii–Moriya Interactions. *Phys. Rev. Lett.* **122**, 257202 (2019).
10. Avci, C. O., Lambert, C.-H., Sala, G. & Gambardella, P. Chiral Coupling between Magnetic Layers with Orthogonal Magnetization. *Phys. Rev. Lett.* **127**, 167202 (2021).
11. Liu, Y., Hou, W., Han, X. & Zang, J. Three-Dimensional Dynamics of a Magnetic Hopfion Driven by Spin Transfer Torque. *Phys. Rev. Lett.* **124**, 127204 (2020).
12. Deger, C. Strain-enhanced Dzyaloshinskii–Moriya interaction at Co/Pt interfaces. *Sci. Rep.* **10**, 12314 (2020).
13. Filianina, M. *Electric field-induced strain control of magnetism in in-plane and out-of-plane magnetized thin films* PhD thesis (Mainz, 2021).
14. Shen, Z. *et al.* Strain tunable skyrmions and strong Dzyaloshinskii–Moriya interaction in two-dimensional Janus Cr(X,Y)₃ trihalides monolayers. *arXiv: 2109.00723 [cond-mat]* (2021).

15. Hirsch, J. E. Spin Hall Effect. *Phys. Rev. Lett.* **83**, 1834–1837 (1999).
16. Miron, I. M. *et al.* Perpendicular switching of a single ferromagnetic layer induced by in-plane current injection. *Nature* **476**, 189–193 (2011).
17. Emori, S., Bauer, U., Ahn, S.-M., Martinez, E. & Beach, G. S. D. Current-driven dynamics of chiral ferromagnetic domain walls. *Nat. Mater.* **12**, 611–616 (2013).
18. Manchon, A. *et al.* Current-induced spin-orbit torques in ferromagnetic and antiferromagnetic systems. *Rev. Mod. Phys.* **91**, 035004 (2019).
19. Karnad, G. V. *et al.* Modification of Dzyaloshinskii-Moriya-Interaction-Stabilized Domain Wall Chirality by Driving Currents. *Phys. Rev. Lett.* **121**, 147203 (2018).
20. Kato, N. *et al.* Current-Induced Modulation of the Interfacial Dzyaloshinskii-Moriya Interaction. *Phys. Rev. Lett.* **122**, 257205 (2019).
21. Freimuth, F., Blügel, S. & Mokrousov, Y. Dynamical and current-induced Dzyaloshinskii-Moriya interaction: Role for damping, gyromagnetism, and current-induced torques in noncollinear magnets. *Phys. Rev. B* **102**, 245411 (2020).
22. Kikuchi, T., Koretsune, T., Arita, R. & Tatara, G. Dzyaloshinskii-Moriya Interaction as a Consequence of a Doppler Shift due to Spin-Orbit-Induced Intrinsic Spin Current. *Phys. Rev. Lett.* **116**, 247201 (2016).
23. Freimuth, F., Blügel, S. & Mokrousov, Y. Relation of the Dzyaloshinskii-Moriya interaction to spin currents and to the spin-orbit field. *Phys. Rev. B* **96**, 054403 (2017).
24. Han, D.-S. *et al.* Asymmetric Hysteresis for Probing Dzyaloshinskii-Moriya Interaction. *Nano Lett.* **16**, 4438–4446 (2016).

- 25. Stamps, R. L. Mechanisms for exchange bias. *J. Phys. D: Appl. Phys.* **33**, R247–R268 (2000).
- 26. Meiklejohn, W. H. & Bean, C. P. New Magnetic Anisotropy. *Phys. Rev.* **105**, 904–913 (1957).
- 27. Slonczewski, J. C. Origin of biquadratic exchange in magnetic multilayers. *Journal of Applied Physics* **73**, 5957–5962 (1993).
- 28. Slonczewski, J. C. Fluctuation mechanism for biquadratic exchange coupling in magnetic multilayers. *Phys. Rev. Lett.* **67**, 3172–3175 (1991).
- 29. Meer, H. *et al.* Direct Imaging of Current-Induced Antiferromagnetic Switching Revealing a Pure Thermomagnetoelastic Switching Mechanism in NiO. *Nano Lett.* **21**, 114–119 (2021).